

Detection and Parameter Extraction of Low Probability of Intercept Frequency Hopping Signals using the Spectrogram and the Reassigned Spectrogram

Daniel L. Stevens¹ and Stephanie A. Schuckers²

¹ Air Force Research Laboratory, Rome, NY

Received: 10 February 2015 Accepted: 1 March 2015 Published: 15 March 2015

Abstract

Digital intercept receivers are currently moving away from Fourier-based analysis and towards classical time-frequency analysis techniques, such as the Wigner-Ville distribution, Choi-Williams distribution, spectrogram, and scalogram, for the purpose of analyzing low probability of intercept radar signals (e.g. triangular modulated frequency modulated continuous wave and frequency shift keying). Although these classical time-frequency techniques are an improvement over the Fourier-based analysis, they still suffer from a lack of readability, due to cross-term interference, and a mediocre performance in low SNR environments. This lack of readability may lead to inaccurate detection and parameter extraction of these radar signals. In this paper, the use of the Hough transform, because of its ability to suppress cross-term interference, separate signals from cross-terms, and perform well in the presence of noise, is proposed as an improved signal analysis technique. With these qualities, the Hough transform has the potential to produce better readability and consequently, more accurate signal detection and parameter extraction metrics.

Index terms— radar detection, hough transform, low probability of intercept.

1 Introduction a) Frequency hopping techniques

low probability of intercept (LPI) radar that uses frequency hopping techniques changes the transmitting frequency in time over a wide bandwidth in order to prevent an intercept receiver from intercepting the waveform. The frequency slots used are chosen from a frequency hopping sequence, and it is this unknown sequence that gives the radar the advantage over the intercept receiver in terms of processing gain. The frequency sequence appears random to the intercept receiver, and so the possibility of it following the changes in frequency is remote [PAC09]. This prevents a jammer from reactively jamming the transmitted frequency [ADA04]. Frequency hopping radar performance depends only slightly on the code used, given that certain properties are met. This allows for a larger variety of codes, making it more difficult to intercept. Though classical time-frequency analysis techniques are a great improvement over Fourier analysis techniques, they may suffer from poor time-frequency localization, as described above. This may result in degraded readability of time-frequency representations, potentially leading to inaccurate LPI radar signal detection and parameter extraction metrics, and as such, can lead to decisions based on inaccurate information.

2 c) Reassignment method

A promising avenue for overcoming this deficiency is the utilization of the reassignment method. The reassignment method, which can be applied to most energy distributions [HIP00], has, in theory, a perfectly localized distribution for chirps, tones and impulses [BOA03], making it a good candidate for the analysis of certain

41 LPI radar signals, such as the triangular modulated frequency modulated continuous wave (FMCW) (which can
42 be viewed as back-to-back chirps) and the frequency shift keying (FSK) (which can be viewed as tones).

43 3 d) Spectrogram and reassigned spectrogram

44 The spectrogram is defined as the magnitude squared of the STFT[BOA03], [HIP00], [HLA92], [MIT01], [PAC09].
45 For non-stationary signals, the STFT is usually in the form of the spectrogram [GRI08].

46 The STFT of a signal $x(t)$ is given in equation 2.5 as: $X(t, \omega) = \int_{-\infty}^{\infty} x(\tau) w(\tau - t) e^{-j\omega(\tau - t)} d\tau$ (2.5)

47 Where $w(t)$ is a short time analysis window localized around $t = 0$ and $\omega = 0$. Because
48 multiplication by the relatively short window $w(t)$ effectively suppresses the signal outside a neighborhood
49 around the analysis point $t = 0$, the STFT is a 'local' spectrum of the signal $x(t)$ around t . Think of the
50 window $w(t)$ as sliding along the signal $x(t)$ and for each shift $w(t - \tau)$ we compute the usual Fourier
51 transform of the product function $x(\tau)w(\tau - t)$. The observation window allows localization of the spectrum
52 in time, but also smears the spectrum in frequency in accordance with the uncertainty principle, leading to a
53 trade-off between time resolution and frequency resolution. In general, if the window is short, the time resolution
54 is good, but the frequency resolution is poor, and if the window is long, the frequency resolution is good, but the
55 time resolution is poor.

56 The STFT was the first tool devised for analyzing a signal in both time and frequency simultaneously. For
57 analysis of human speech, the main method was, and still is, the STFT. In general, the STFT is still the most
58 widely used method for studying non-stationary signals [COH95].

59 The spectrogram (the squared modulus of the STFT) is given by equation 2.6 as: $S(t, \omega) = |X(t, \omega)|^2$ (2.6)

60 The spectrogram is a real-valued and nonnegative distribution. Since the window w of the STFT is assumed
61 of unit energy, the spectrogram satisfies the global energy distribution property. Thus we can interpret the
62 spectrogram as a measure of the energy of the signal contained in the time-frequency domain centered on the
63 point (t, f) and whose shape is independent of this localization.

64 Here are some properties of the spectrogram: 1) time and frequency covariance -the spectrogram preserves time
65 and frequency shifts, thus the spectrogram is an element of the class of quadratic time-frequency distributions
66 that are covariant by translation in time and in frequency (i.e. Cohen's class); 2) time-frequency resolution -the
67 time-frequency resolution of the spectrogram is limited exactly as it is for the STFT; there is a trade-off between
68 time resolution and frequency resolution. This poor resolution is the main drawback of this representation; 3)
69 interference structure -as it is a quadratic (or bilinear) representation, the spectrogram of the sum of two signals
70 is not the sum of the two spectrograms (quadratic superposition principle); there is a crossspectrogram part and a
71 real part. Thus, as for every quadratic distribution, the spectrogram presents interference terms; however, those
72 interference terms are restricted to those regions of the time-frequency plane where the signals overlap. Thus if
73 the signal components are sufficiently distant so that their spectrograms do not overlap significantly, then the
74 interference term will nearly be identically zero[COH95], [HLA92], [ISI96].

75 The original idea of reassignment was introduced in an attempt to improve the spectrogram [OZD03]. As
76 with any other bilinear energy distribution, the spectrogram is faced with an unavoidable trade-off between the
77 reduction of misleading interference terms and a sharp localization of the signal components.

80 4 Global Journal of Researches in Engineering () Volume XX 81 Issue IV Version I 13

82 Year 2020F © 2020 Global Journals

83 We can define the spectrogram as a twodimensional convolution of the WVD of the signal by the WVD of the
84 analysis window, as in equation 2.9: $S(t, \omega) = \int_{-\infty}^{\infty} \int_{-\infty}^{\infty} W(t, \omega, \tau, \omega') X(t, \omega, \tau) X^*(t, \omega', \tau) d\tau$ (2.9)

85 Therefore, the distribution reduces the interference terms of the signal's WVD, but at the expense of time
86 and frequency localization. However, a closer look at equation 2.9 shows that (t, ω) delimits a time-frequency domain at the vicinity of the (t, ω) point, inside which a weighted average of
87 the signal's WVD values is performed. The key point of the reassignment principle is that these values have no
88 reason to be symmetrically distributed around (t, ω) , which is the geometrical center of this domain.
89 Therefore, their average should not be assigned at this point, but rather at the center of gravity of this domain,
90 which is much more representative of the local energy distribution of the signal [BOA03]. Reasoning with a
91 mechanical analogy, the local energy distribution $S(t, \omega)$ (as a function of
92 t and ω) can be considered as a mass distribution, and it is much more accurate to assign the total mass (i.e.
93 the spectrogram value) to the center of gravity of the domain rather than to its geometrical center. Another way
94 to look at it is this: the total mass of an object is assigned to its geometrical center, an arbitrary point which
95 except in the very specific case of a homogeneous distribution, has no reason to suit the actual distribution. A
96 much more meaningful choice is to assign the total mass of an object, as well as the spectrogram value, to the
97 center of gravity of their respective distribution [BOA03]. This is exactly how the reassignment method proceeds:
98 it moves each value of the spectrogram computed at any point (t, ω) to another point (t, ω)

162 was noted (here 98%, 78%, 75%, 63%), and the lowest of these 4 values was recorded (63%). Ten test runs were
163 performed for both timefrequency analysis tools (spectrogram and reassigned spectrogram) for this waveform.
164 The average of these recorded low values was determined and then assigned as the threshold for that particular
165 time-frequency analysis tool. Note -the threshold value assigned for the spectrogram was 60%. For percent
166 detection determination, these threshold values were included in the time-frequency plot algorithms so that the
167 thresholds could be applied automatically during the plotting process. From the threshold plot, the signal was
168 declared a detection if any portion of each of the signal components was visible (see Figure 2). Modulation
169 bandwidth: Distance from highest frequency value of signal (at a threshold of 20% maximum intensity) to lowest
170 frequency value of signal (at same threshold) in Y-direction (frequency).

171 7 Global Journal of Researches in Engineering

172 The threshold percentage was determined based on manual measurement of the modulation bandwidth of the
173 signal in the time-frequency representation. This was accomplished for ten test runs of each time-frequency
174 analysis tool (spectrogram and reassigned spectrogram), for the 4 component frequency hopping waveform.
175 During each manual measurement, the max intensity of the high and low measuring points was recorded. The
176 average of the max intensity values for these test runs was 20%. This was adopted as the threshold value,
177 and is representative of what is obtained when performing manual measurements. This 20% threshold was also
178 implemented for determining the modulation period and the time-frequency localization (both are described
179 below).

180 For modulation bandwidth determination, the 20% threshold value was included in the time-frequency plot
181 algorithms so that the threshold could be applied automatically during the plotting process. From the threshold
182 plot, the modulation bandwidth was manually measured (see Figure ??). From this threshold plot, the modulation
183 period was measured manually from the left side of the signal (left red arrow) to the right side of the signal (right
184 red arrow) in the x-direction (time). This was done for all 4 signal components, and the average value was
185 determined.

186 Time-frequency localization: From Figure 6, the time-frequency localization is a manual measurement (at a
187 threshold of 20% maximum intensity) of the 'thickness' (in the y-direction) of the center of each of the 4 frequency
188 hopping signal components, and then the average of the 4 values are determined. The average frequency 'thickness'
189 is then converted to: percent of the entire y-axis. Lowest detectable SNR: The lowest SNR level at which at
190 least a portion of each of the signal components exceeded the set threshold listed in the percent detection section
191 above.

192 For lowest detectable SNR determination, these threshold values were included in the time-frequency plot
193 algorithms so that the thresholds could be applied automatically during the plotting process. From the threshold
194 plot, the signal was declared a detection if any portion of each of the signal components was visible.

195 The lowest SNR level for which the signal was declared a detection is the lowest detectable SNR (see Figure
196 ??).

197 The data from all 100 runs for each test was used to produce the actual, error, and percent error for each of
198 these metrics listed above.

199 The metrics from the spectrogram were then compared to the metrics from the reassigned spectrogram. By
200 and large, the reassigned spectrogram outperformed the spectrogram, as will be shown in the results section. 1,
201 the reassigned spectrogram outperformed the spectrogram in average percent error: carrier frequency (0.74% vs.
202 0.93%), modulation bandwidth (10.82% vs. 25.70%), modulation period (9.30% vs. 11.84%), and time-frequency
203 localization (ydirection) (4.05% vs. 9.09%);and in average: percent detection (86.84% vs. 67.24%), and lowest
204 detectable SNR (-3.5db vs. -2.7db), while the spectrogram outperformed the reassigned spectrogram in average
205 plot time (4.72s vs. 7.62s).

206 Figure ?? shows comparative plots of the spectrogram vs. the reassigned spectrogram (4 component frequency
207 hopping) at SNRs of 10dB (top), 0dB (middle), and -3dB (bottom). IV.

208 8 Discussion

209 This section will elaborate on the results from the previous section.

210 From Table 1, the performance of the spectrogram and the reassigned spectrogram will be summarized,
211 including strengths, weaknesses, and generic scenarios in which each particular signal analysis tool might be
212 used.

213 The spectrogram outperformed the reassigned spectrogram in average plot time (4.72s vs 7.62s). However, the
214 spectrogram was outperformed by the reassigned spectrogram in every other category. The spectrogram's extreme
215 reduction of cross-term interference is grounds for its good plot time, but at the expense of signal localization (i.e.
216 it produces a 'thicker' signal (as is seen in Figure ??) -due to the trade-off between cross-term interference and
217 signal localization). This poor signal localization ('thicker' signal), coupled with the reassigned spectrogram's
218 'squeezing' quality, can account for the spectrogram being outperformed by the reassigned spectrogram in the
219 areas of: average percent error of modulation bandwidth, modulation period, time-frequency localization (y-
220 direction), lowest detectable SNR, and percent detection. Note that average percent detection and lowest
221 detectable SNR are both based on visual detection in the time-frequency representation. Figure ?? clearly

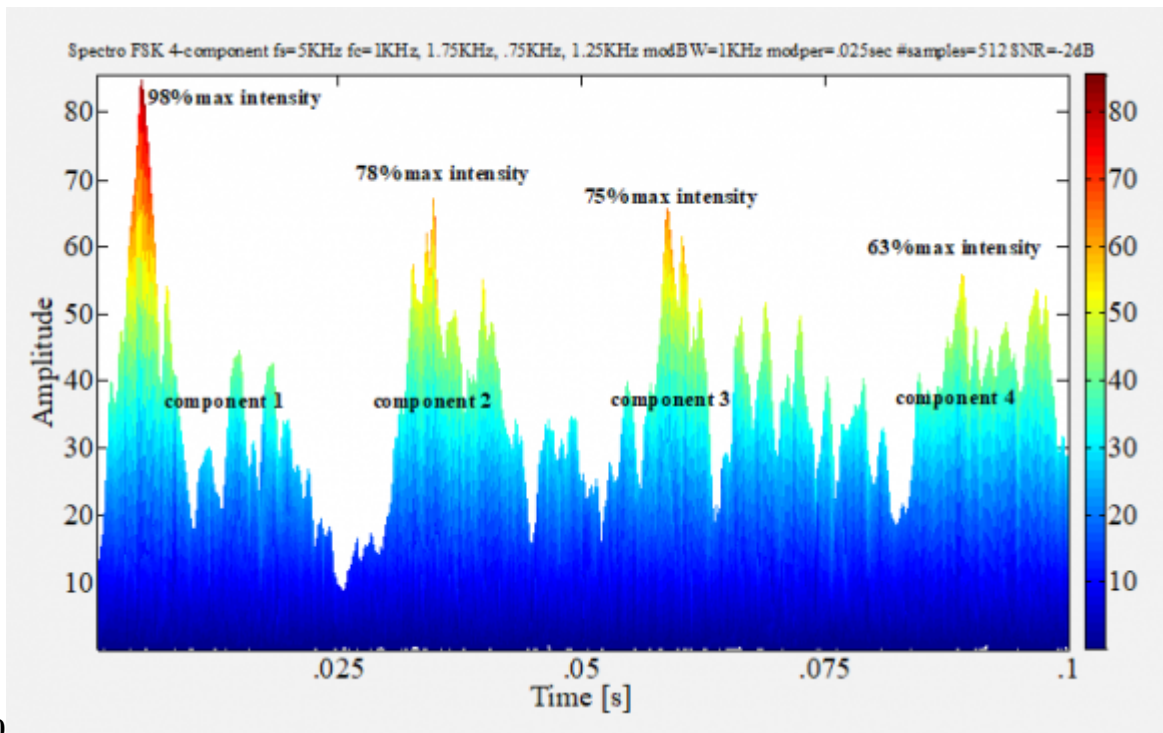
222 shows that the signals in the reassigned spectrogram plots are more readable than those in the spectrogram
 223 plots, which accounts for the reassigned spectrogram's better average percent detection and lowest detectable
 224 SNR. The spectrogram might be used in a scenario where a short plot time is necessary, but where accurate
 225 parameters are not as vital. Such a scenario might be a 'quick and dirty' check to see if a signal is present,
 226 without accurate extraction of its parameters. The reassigned spectrogram might be used in a scenario where
 227 you need accurate parameters, in a low SNR environment, in a quick time frame.

228 V.

229 9 Conclusions

230 Digital intercept receivers, whose main job is to detect and extract parameters from low probability of intercept
 231 radar signals, are currently moving away from Fourier-based analysis and towards classical timefrequency analysis
 232 techniques, such as the spectrogram, for the purpose of analyzing low probability of intercept radar signals. Based
 233 on the research performed for this paper (the novel direct comparison of the spectrogram versus the reassigned
 234 spectrogram for the signal analysis of low probability of intercept frequency hopping radar signals) it was shown
 235 that the reassigned spectrogram by-and-large outperformed the spectrogram in analyzing these low probability of
 236 intercept radar signals -for reasons brought out in the discussion section above. More accurate characterization
 237 metrics could well translate into saved equipment and lives.

238 Future plans include analysis of additional low probability of intercept radar waveforms, using additional
 time-frequency analysis and reassignment method techniques. ¹



2020

Figure 1: Year 2020 F©

239

¹© 2020 Global Journals

9 CONCLUSIONS

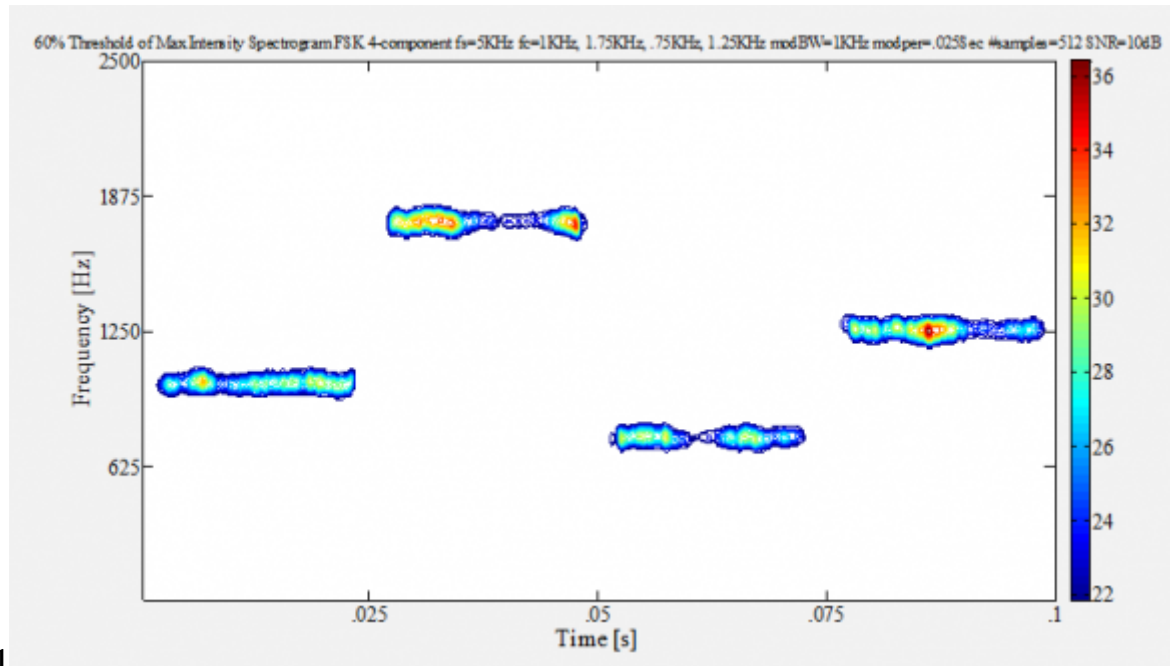


Figure 2: Figure 1 :

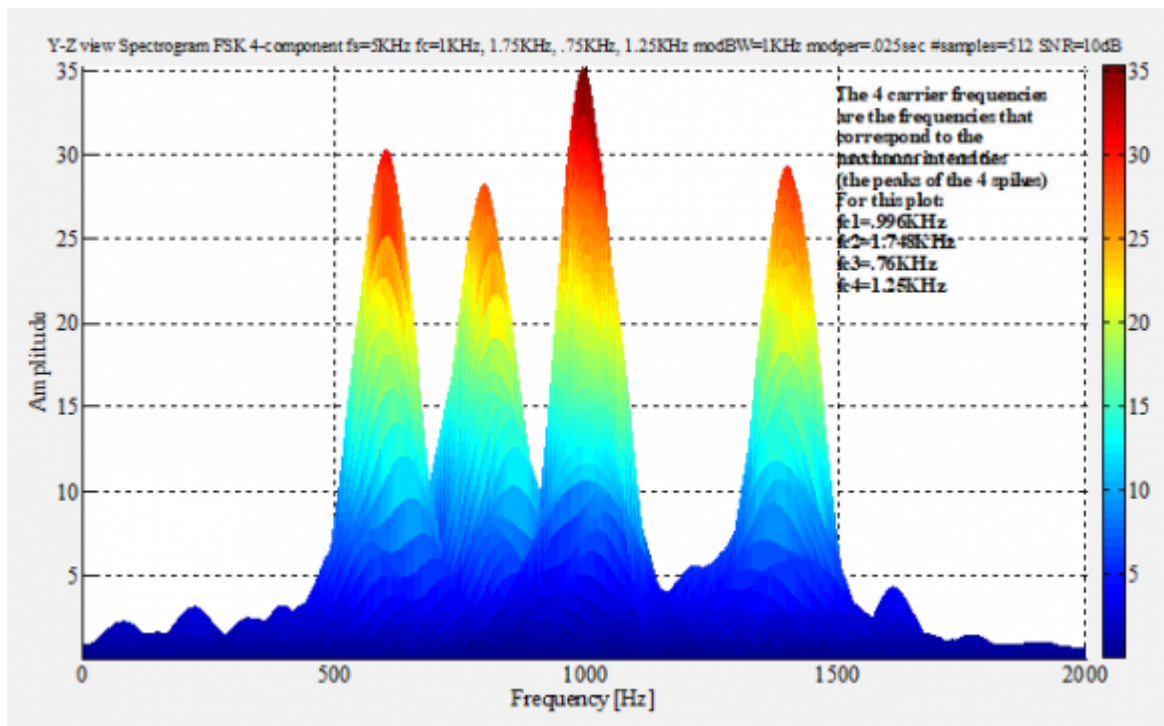


Figure 3: (

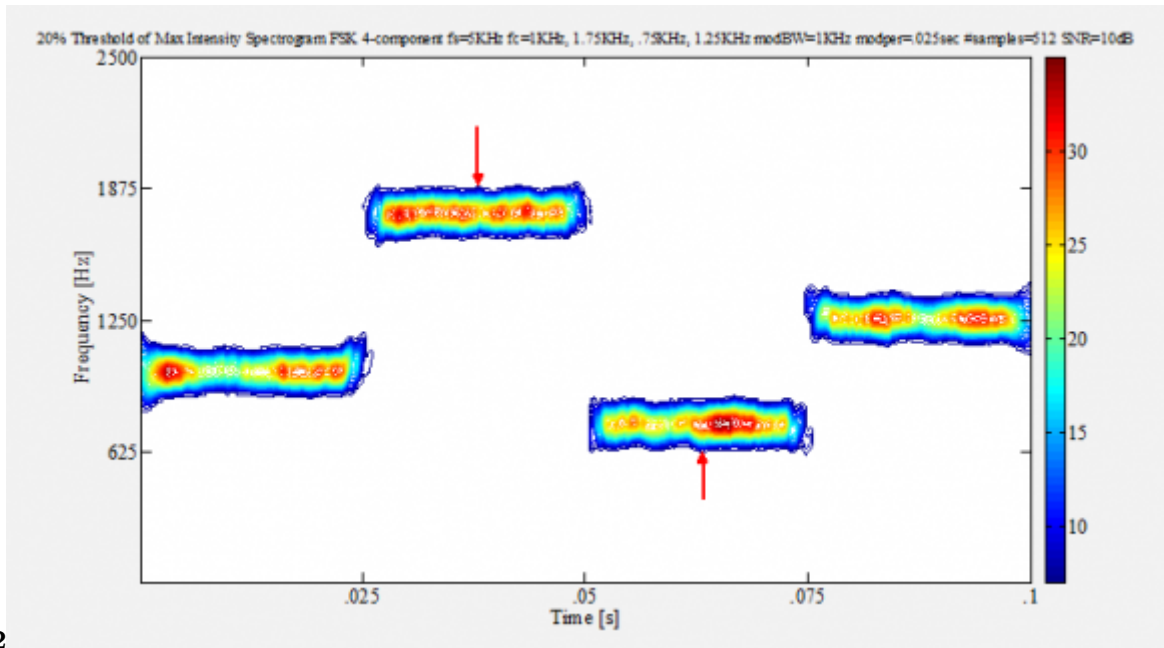


Figure 4: Figure 2 :

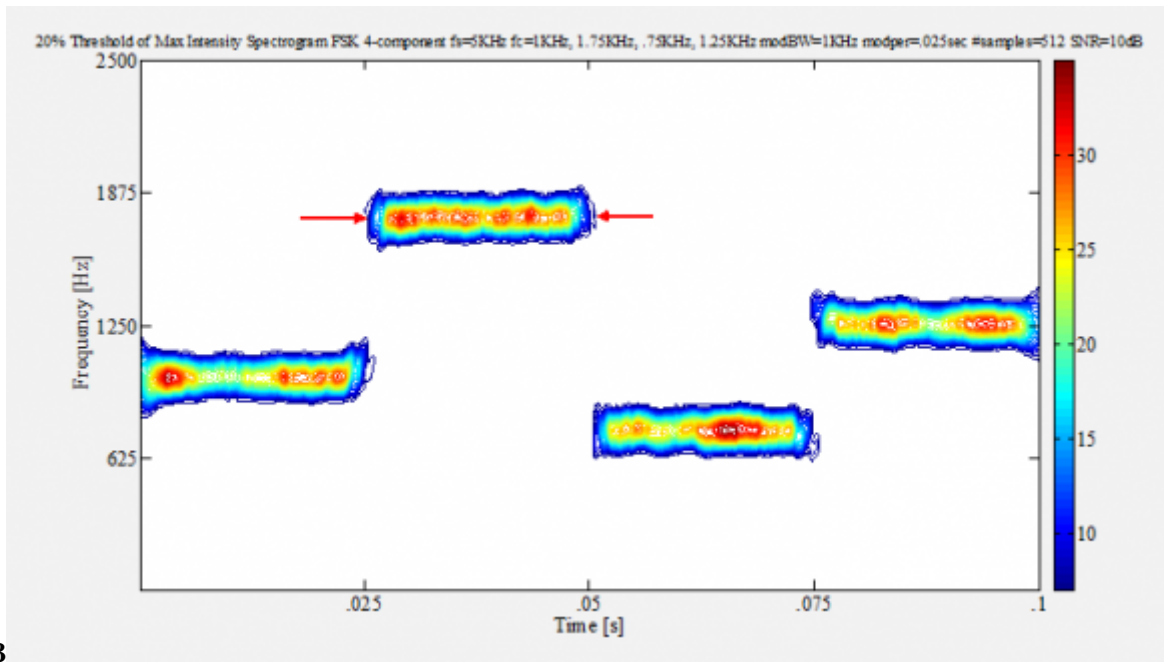


Figure 5: Figure 3 :

9 CONCLUSIONS

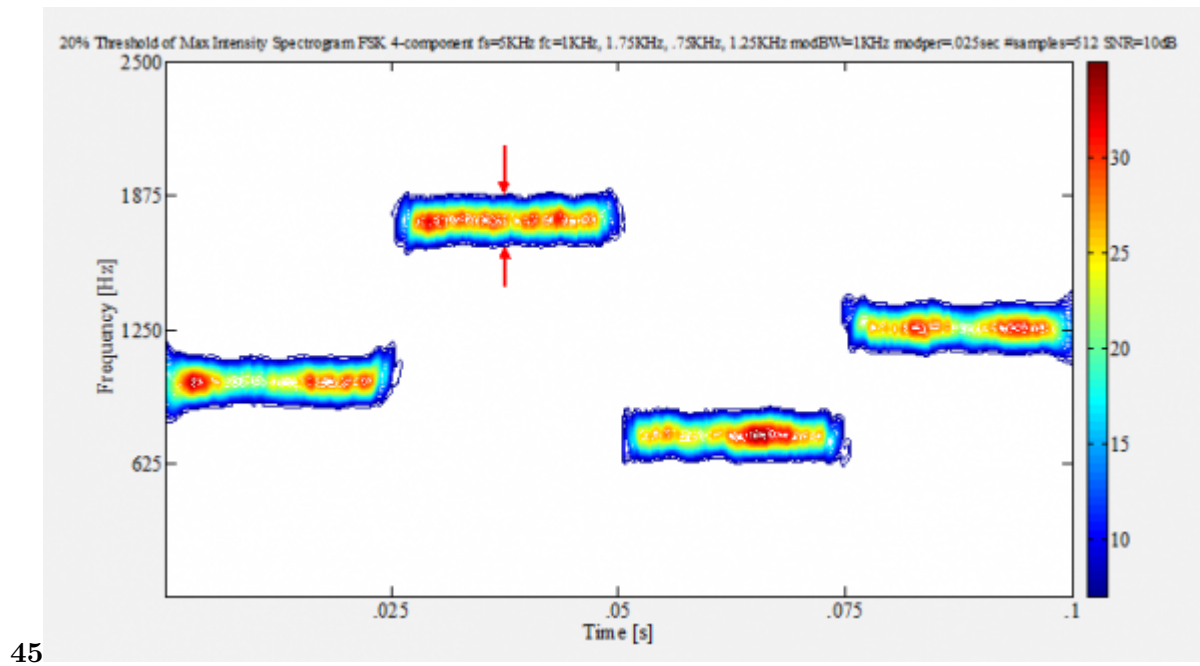


Figure 6: Figure 4 :Figure 5 :

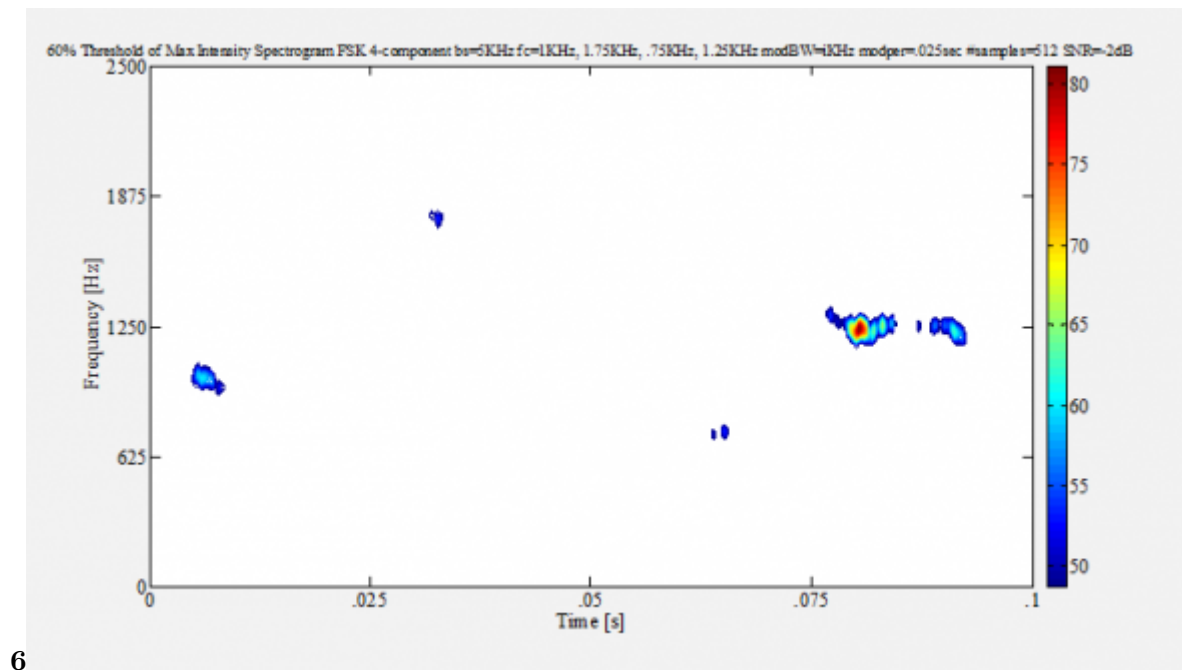


Figure 7: Figure 6 :

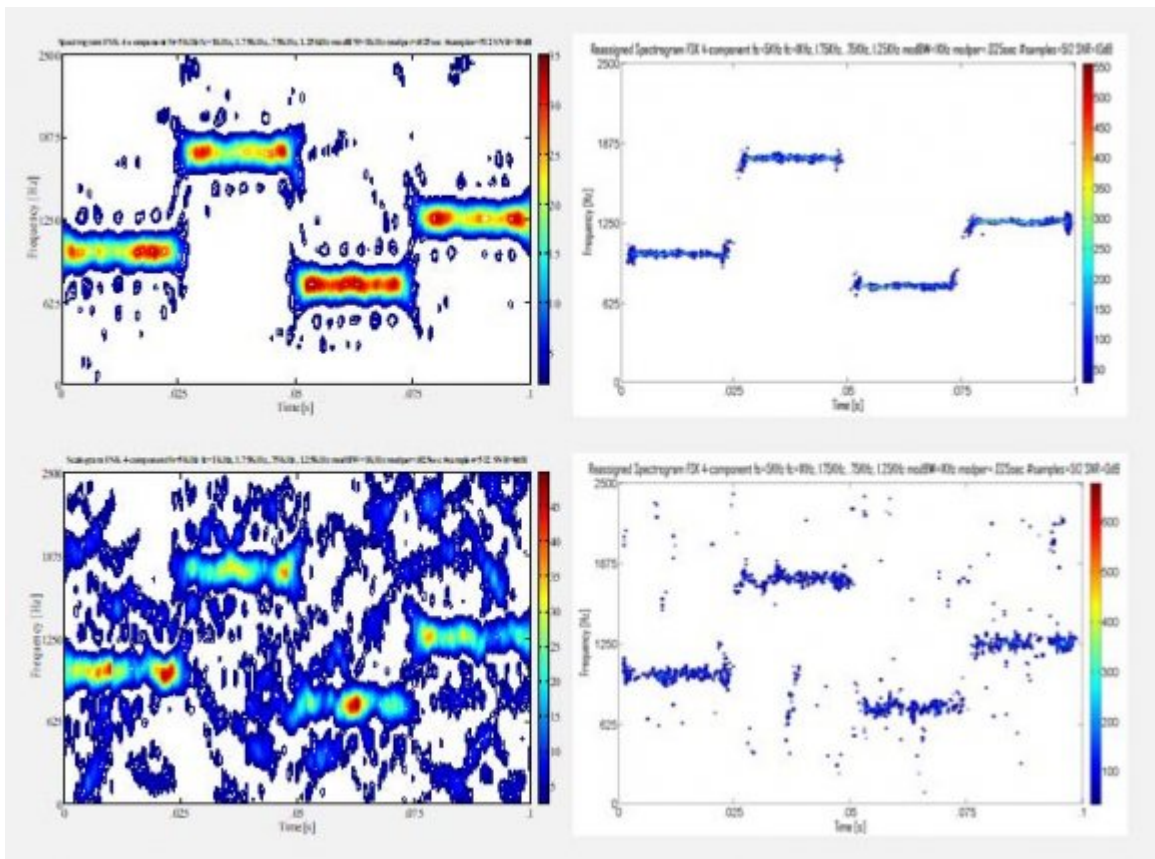
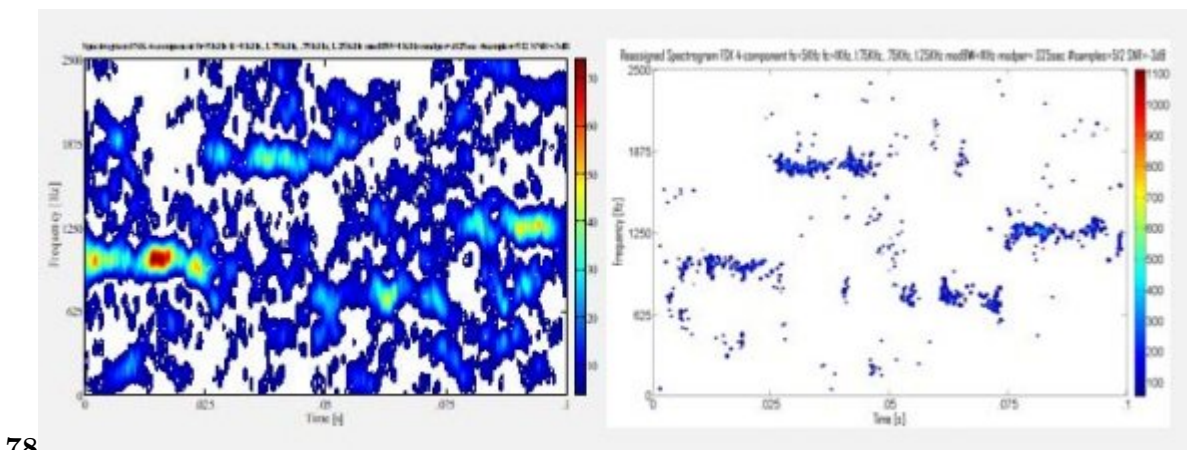


Figure 8:



78

Figure 9: Figure 7 :Figure 8 :

1

presents the overall test metrics for the signal processing analysis techniques used in this testing (spectrogram versus assigned spectrogram).

Figure 10: Table 1

1

carrier frequency	0.93%	0.74%
modulation bandwidth	25.70%	10.82%
modulation period	11.84%	9.30%
time-frequency localization-y	9.09%	4.05%
percent detection	67.24%	86.84%
lowest detectable snr	-2.7db	-3.5db
plotime	4.72s	7.62s
From Table		

Figure 11: Table 1 :

-
- 240 [Xia and Chen (1999)] ‘A Quantitative SNR Analysis for the Pseudo Wigner-Ville Distribution’. X Xia , V Chen
241 . *IEEE Transactions on Signal Processing* October, 1999. 47 (10) p. .
- 242 [Wei et al. (2003)] ‘Analysis of Multicomponent LFM Signals Using Time-Frequency and The Gray-Scale Inverse
243 Hough Transform’. G Wei , S Wu , E Mao . *IEEE Workshop on Statistical Signal Processing* September 28
244 -October 1, 2003. p. .
- 245 [Conference Record of the Twenty-Eighth Asilomar Conference on Signals, Systems and Computers ()]
246 *Conference Record of the Twenty-Eighth Asilomar Conference on Signals, Systems and Computers*,
247 1994. p. .
- 248 [Pac09] ace ())b6 *Detecting and Classifying Low Probability of Intercept Radar*, [Pac09] Pace , P . 2009. Norwood,
249 MA: Artech House.
- 250 [Papandreou et al.] *Detection and Estimation of Generalized Chirps Using Time-Frequency Representations*, A
251 Papandreou , G F Boudreaux-Bartels , S Kay .
- 252 [Mitra ()] *Digital Signal Processing, A Computer-Based Approach, Second Edition*, S Mitra . 2001. Boston, MA:
253 McGraw-Hill.
- 254 [Rangayyan and Krishnan ()] ‘Feature Identification in the Time-Frequency Plane by Using the Hough-Radon
255 Transform’. R Rangayyan , S Krishnan . *Pattern Recognition* 2001. 34 p. .
- 256 [Li and Bi ()] X Li , G Bi . *A New Reassigned Time-Frequency Representation. 16 th European Signal Processing*
257 *Conference*, (Lausanne, Switzerland) August 25-29, 2008. p. .
- 258 [Hlawatsch and Boudreaux-Bartels (1992)] ‘Linear and Quadratic Time-Frequency Signal Representations’. F
259 Hlawatsch , G F Boudreaux-Bartels . *IEEE Signal Processing Mag* April 1992. 9 (2) p. .
- 260 [Li and Xiao (2003)] ‘Recursive Filtering Radon-Ambiguity Transform Algorithm for Detecting Multi-LFM
261 Signals’. Y Li , X Xiao . *Journal of Electronics (China)* May 2003. 20 (3) p. .
- 262 [Ozd03] zdemir (2003)]b5 *Time-Frequency Component Analyzer. Dissertation*, [Ozd03] Ozdemir , A . Sept. 2003.
263 Ankara, Turkey. Bilkent University
- 264 [Auger et al. ()] *Time-Frequency Toolbox Users Manual*, F Auger , P Flandrin , P Goncalves , O Lemoine . 1996.
265 Centre National de la Recherche Scientifique and Rice University